

SHIELDING CALCULATIONS FOR THE ANTIPROTON TARGET AREA

J. D. Cossairt and P. Yurista

September 1982

1. Introduction

This TM summarizes shielding calculations performed in conjunction with the design of the antiproton target hall. The following radiological considerations were examined: soil activation, residual activity of components, and beam-on radiation. In addition, at the request of the designers, the energy deposition in the proposed graphite beam dump was examined for several targeting conditions in order to qualitatively determine its ability to survive. Such estimates were not made for the tungsten target in the present work. Such considerations have been made elsewhere.¹

The question of soil activation has been addressed in previous reports.^{2,3} In this respect in the present work we are covering old territory. However, the target station has now been relocated from the location designed in 1978 at F25 to a new enclosure to be located near F17. The design of this enclosure has now been substantially altered and many details not available for the authors of Refs. 1 and 2 have

been refined to the point where the new calculations reported here were needed.

As is usual practice at Fermilab, the code CASIM by A. Van Ginneken⁴ was used to do these calculations using Monte-Carlo techniques. In all cases the following targeting conditions were modeled for the incident protons:

Energy: 125 GeV

Lower momentum cutoff: 0.3 GeV/c

Target: 2.54 cm x 2.54 cm x 5 cm long (tungsten)

Dump dimension: 15.24 x 15.24 x 183 cm long (graphite)

Spot size at target: (see below) typically 0.1 mm sigma

Intensity: 3×10^{12} protons/sec

Figures 1 and 2 show the architectural drawings of this area as they exist at the present time. The bulk shielding is also shown here and this was the quantity of shielding assumed to be present in this work. It should be pointed out that the validity of these results has an inverse relationship with the number of voids and their volume which will inevitably appear in the course of actually rigging in the shielding. Thus the final shielding can be expected to be slightly less effective than would be the idealized shielding in the drawings.

2. Soil Activation Calculations

In comparison with the situation at the F25 location reviewed in Refs. 2 and 3 the principal difference at F17 is the enlarged width of the pit (9 ft inside width) and the fact that at F17 no bathtub is being designed. The exact rectangular design was modeled and a listing of the FORTRAN geometry code is included here as Table 1. In this code, the different shielding materials are denoted as follows:

N=0; void

N=1; tungsten

N=2; iron

N=3; concrete (density = 2.4 g/cm^3) and protected soil

N=4; graphite (density = 2 g/cm^3)

N=5; "unprotected" soil (density = 2.4 g/cm^3)

It is realized that the density of the soil which is external to the enclosure is typically $2\text{-}2.2 \text{ g/cm}^3$. However elevating this density to 2.4 should improve somewhat the statistics of the Monte-Carlo the stars in the soil subject to groundwater migration to the aquifer without making any nonphysical changes in the results. For purposes of this calculation a zone of 3' extending radially from the outside

of the enclosure walls into the soil was chosen to be a region where activated groundwater would be drained by the sumps and hence be prevented from migrating to the aquifer. The outer boundary of this zone separates "protected" soil from the "unprotected" soil containing radionuclides subject to such migration. For this zone to actually provide the calculated protection it must be drained by underdrains at the bottom of it separated by no more than 6 feet laterally. The code was run with a modification which summed the total star production by particles exceeding the momentum cutoff in each of the five materials. For this soil activation calculation, the protected soil was considered to be part of the concrete while the unprotected soil was counted as a separate material. The beam profile was chosen to be a rectangular Gaussian with a sigma value of 0.1 mm in both transverse coordinates. Two different random number seeds were utilized. Each seed was run both considering "protected" soil to be defined as above and also considering all soil external to the enclosure to be unprotected. This serves to provide an estimate of the amount of activity protected by the proper operation of the underdrain and sump system. The integral of the star density over the appropriate volumes in units of stars/incident proton are as follows (one sigma statistical uncertainties are given):

	Seed 1	Seed 2	Average
Stars/proton outside of enclosure	(9.8±0.8)E-03	(1.2±0.1)E-02	(1.06±0.06)E-02
Stars/proton in unprotected soil	(1.2±0.3)E-03	(3.0±0.4)E-03	(1.84±0.24)E-03

At this point Ref. 2 will be the guide as to the conversion of these star densities to total activities in Curies and then to concentrations of ^3H and ^{22}Na in the drinking water of an off-site individual who is a sole user of a well and who draws 40 gallons per day. Assuming all the migrating activity goes to this single user, this is the standard Fermilab model. Under maximal targeting conditions stated in April, 1982 of 3×10^{12} protons per second,⁵ this would mean 5.4×10^{19} protons per 5000 hr running period. This is a very conservative (high) estimate of the number of protons to be targeted and would represent a grand achievement in accelerator technology by all groups concerned! The result of Ref. 2 was that 7.1 pCi/ml of ^3H and 0.05 pCi/ml of ^{22}Na would be produced by 30.7×10^{-4} stars/proton times 4.8×10^{19} protons/year. We thus have (relying on Ref. 2 to convert from stars to concentrations at the top of the well):

^3H : 1 pCi/ml per 2.07×10^{16} stars

^{22}Na : 1 pCi/ml per 2.95×10^{18} stars

Thus in such a running period one has resulting concentrations in the drinking water of:

$${}^3\text{H}: 4.8 \text{ pCi/ml}$$

$${}^{22}\text{Na}: 0.03 \text{ pCi/ml}$$

due to release of the activity produced in the unprotected soil. Since the concentration guide limits these values to 20 pCi/ml for ${}^3\text{H}$ and 0.2 pCi/ml for ${}^{22}\text{Na}$, the above results in $\frac{4.8}{20} + \frac{0.03}{0.2} = 0.39$ or 39% of the allowable

concentration. Considering the total activity outside of the enclosure in a similar manner, one obtains:

$${}^3\text{H}: 28 \text{ pCi/ml}$$

$${}^{22}\text{Na}: 0.2 \text{ pCi/ml}$$

which when summed, would be 240 per cent of the concentration guides. Thus even if the sumps and underdrains fail completely, the concentration guides would be exceeded by less than a factor of three. The groundwater protection is thus adequate, even if the shielding, because of cracks and small voids, is less effective than the idealized version modified.

3. Residual Activity

The combination of a very high intensity proton beam and high atomic number target obviously lead to high levels of residual activity. These levels are difficult to estimate but various approximations will be used to attempt it here. The determination of incident flux density is crucial here. In Ref. 4 are given conversion factors of stars/cm³ to incident hadron flux (cm⁻²) for cases of thick shields where the internuclear cascade is reaching an equilibrium spectrum. Of course, when one is dealing with the target itself, where one is concerned with the initial interactions of the primary beam, one may simply form the product of star density and absorption interaction length:

$$\text{flux density (cm}^{-2}\text{)} = (\text{stars cm}^{-3}\text{)}\lambda(\text{cm})$$

to obtain this quantity. For example, the tungsten target in the calculations done here has an average star density of 5×10^{-2} stars cm⁻³ per proton. The flux density is thus $5 \times 10^{-2} \times 10 \text{ cm} = 0.5 \text{ cm}^{-2}$ per proton, using 10 cm as the absorption length of tungsten. A reference useful for estimating residual activities is that of Barbier.⁶ This author calculates curves of a quantity called the "danger parameter" some of which are reproduced in Chapter 12 of the Fermilab Radiation Guide. These "danger parameter" curves relate the dose in mrad/hr to the hadron flux density

incident on an infinite slab of a particular material. The values of mrad/hr are given as a function of time after the beam is turned off for different irradiation time periods. Fig. 3 includes such curves for tungsten, copper, and for carbon (the dump). To convert the values obtained from these curves to real exposure rates, one must first multiply the "danger parameter" by the incident flux density and then multiply by the fractional solid angle subtended by the hot object at the location of interest. An example will illustrate this procedure. The target was modeled to be a 2.5 cm square by 5 cm long rectangular solid of tungsten and as calculated above, the average hadron flux density on it would be:

$$0.5 \text{ hadrons cm}^{-2} \text{ per proton}$$

If we have targeting, as above, of 3×10^{12} protons/sec, we thus have a flux of $1.5 \times 10^{12} \text{ cm}^{-2} \text{ sec}^{-1}$. For an irradiation of 360 days and zero cooldown time the danger parameter is about $10^{-4} \text{ mrad hr}^{-1}$ per unit flux density. At one meter such a target subtends no more than $2.5 \text{ cm} \times 5 \text{ cm} / (100 \text{ cm})^2 = 1.3 \times 10^{-3}$ steradian of solid angle or $\frac{0.0013}{4\pi}$ = 1×10^{-4} fractional solid angle. The exposure rate then would be:

$$10^{-4} \times 1.5 \times 10^{12} \times 10^{-4} = 1.5 \times 10^4 \text{ mrad/hr}$$

(solid angle) x (flux density) x (danger parameter)

or 15 rad/hr, a figure which is not out of line with other

experience with Fermilab targets. After one day of cooldown we may expect (from the curves) a reduction by decay of a factor of about 2.5. After 3 months such a target would be down to 1/30 of its initial value or about 500 mrem/hr at one meter. This target will obviously warrant the special handling techniques presently being designed.

The upstream face of the graphite dump and surrounding steel shielding may still be regarded as being struck by incident primaries since the target is relatively thin ($\sim 0.5\lambda$). The average star density over the face is approximately 2×10^{-4} stars/(cm³/proton) which implies a flux of 3×10^{10} cm⁻² sec⁻¹. The carbon danger parameter curve indicates a value of perhaps 2×10^{-5} mrad/hr per unit flux but because of the steel surrounding the graphite a value of 6×10^{-5} (360 day bombardment with no cooloff) would be reasonable for the dump still imbedded in its steel shielding. Here we may consider a 60 cm diameter circle viewed from 100 cm away so that the fractional solid angle is 0.02. The initial dose rate would be (assuming no other sources are present):

$$0.02 \times 6 \times 10^{-5} \times 3 \times 10^{10} = 36000 \text{ mrad/hr}$$

It should be noted that this is for the isolated graphite in place in its steel surroundings and neglects contribution from the walls which, in effect, increase the solid angle.

If the dump is removed and is out by itself the danger parameter after a 360 day run with zero cooldown is reduced to about 2×10^{-5} . The fractional solid angle of the face of the dump at one meter is 0.002. In about two hours of cooloff, the decay is about a factor of 20 so that the dose rate of one meter would be about 60 mrad per hour at one meter after even this short cooldown period. The graphite dump is thus quite manageable. This difference is due to the dominance of ^{11}C (half-life=20 min.) and ^7Be (half-life=53 days) in the activated dump as compared with many radionuclides of half-lives of one year or longer produced in the steel and tungsten objects. The star densities found on the lower (hottest) ends of the elevator segments are reduced by one to two orders of magnitude below the "straight-ahead" levels. Thus, an elevator segment viewed individually from the end should not be much hotter than 20 rads/hr at one meter. The top of the elevator segments, will have less residual radioactivity by several (about 8) orders of magnitude. Again, the high level of the steel components will require special handling techniques.

4. Beam-On Dose Rates in Above Ground Areas

The above ground dose rates were estimated using CASIM for 3 separate areas. These were the outdoor area over the transport tunnel from the Main Ring, the exclusion area directly over the target and dump region, and the area adjacent to the exclusion area which looks at the target on a diagonal plane relative to the vertical direction. For these cases cylindrical approximations to the geometry were made in that each interface between material became the radius of concentric cylinder. Figures 4, 5, and 6 show the geometries specified in FORTRAN for these three situations.

For the case of the beam transport enclosure, the scrape at 8 milliradians of a 0.5 cm sigma beam spot incident on the inner pipe wall of a magnet the size of two EPB dipoles followed by a quadrupole was modeled. Fig. 4 also shows a contour plot of equal star densities as a function of longitudinal coordinate Z and radius R. As one can see, after 18.5 ft of shielding (563 cm), one has a star density of, at worst, 10^{-12} stars $\text{cm}^{-3}/\text{proton}$ at the maximum intensity of 3×10^{12} p/sec and using a conversion of 10^{-2} mrem cm^3/star , one obtains a accident condition equivalent rate of:

$$1 \times 10^{-12} \frac{\text{star}}{\text{cm}^3 \text{p}} \times 3 \times 10^{12} \frac{\text{p}}{\text{sec}} \times 10^{-2} \frac{\text{mrem}}{\text{star}} \times \frac{3600 \text{ sec}}{\text{hr}} = 108 \frac{\text{mrem}}{\text{hr}}$$

Under the Fermilab Radiation Guide, the area above these transport enclosures will require fencing. This is reasonable since it has minimal occupancy.

The case of the area directly over the target and dump assembly inside the service building is likewise shown as modeled in Fig. 5 where, again, a contour plot of the CASIM results is included. Again a maximum star density of 10^{-12} stars $\text{cm}^{-3}/\text{proton}$ is found. This would imply the same dose equivalent rate as above, approximately 100 mrem/hr. Because of cracks and penetrations, this estimate is likely to be somewhat low so that this area has been designated as an exclusion area by the designers and will be interlocked, since the above is a continuous dose rate during operations. It will have a nine foot high shielding block wall surrounding it (not shown in Figs. 1 & 2).

Fig. 6 is a cross section showing the diagonal line between the beam axis and the area adjacent to the exclusion area mentioned above. As in the above, a cylindrical model was used and the results are shown in Fig. 7. The cascade maximum results in a star density of 10^{-13} stars $\text{cm}^{-3}/\text{proton}$ so that the dose equivalent rate with continuous 3×10^{12} p/sec on target becomes 10 mrem/hr.

This is acceptable for an area posted as a radiation area having minimal occupancy (not offices or workbenches!), according to the Fermilab Radiation Guide. To obtain unrestricted occupancy, one could apply additional shielding at the corner to get this dose down to less than 0.25 mrem per hour. This factor of forty could be achieved with about 5 ft. of concrete shielding or by judicious placement of heavy power supplies and the shield block walls. It is possible that skyshine over the top of the exclusion area can contribute some exposure in this area. This is difficult to estimate but could be fixed by a shielding block roof installed over the shield block wall. It is clear that these areas are designed with small margins for error and with no safety factors included in the above. Also extensive radiation surveys will be required. A risk is being taken that modifications to the above ground areas may be needed "after the fact."

5. Calculations of Energy Deposition in the Graphite Beam Dumps

At the request of the designers, one of the authors (JDC) calculated the distribution of energy deposition in the graphite dump in order to qualitatively determine its potential survivability. This was done for 2 cases of beam spot size at the tungsten target; one having a sigma of 0.01 cm and another having a sigma of 0.038 cm (Gaussian profiles). Figs. 8 and 9 are plots of energy deposition in units of Joules/gram as a function of depth (Z) for the different spot sizes averaged over indicated radial bins. The proton intensity was taken to be 3×10^{12} protons/spill. In these Figs., the bumps at $Z \sim 180$ is due to the transition from graphite to the steel (larger atomic number) at the end of the dump. With the smaller spot size, energy densities of up to 400 or 500 Joules/gm per 3×10^{12} protons can be expected. The larger spot size produces energy deposition values an order of magnitude smaller. Fig. 10 is copied from the Ref. 1 and gives plots of this energy deposition density versus temperature in various target materials. The curve for graphite indicates that the dump will rise to a temperature well below its sublimation point of 3652 °C.

As one can see, small values of approximately 10 Joules/gram per 3×10^{12} protons are achieved at radii of four times the sigma. Such smaller values are also obtained at the Z corresponding to the end of the dump. It thus appears that this beam dump will survive individual beam bursts. Studies of long term effects of continuous deposition of such energies have not been made here but the results calculated here may be useful input for such estimates.

References

1. The Fermilab Antiproton Source Design Report, Second Edition, June, 1981.
2. P. J. Gollon, "Soil Activation Calculations for the Anti-proton Target Area," TM-816, September, 1978.
3. C. V. Canada, "An Updated Review of Soil Radioactivation Calculations for the Anti-proton Target Area," TM-1023, December, 1980.
4. A. Van Ginneken and M. Awschalom, "High Energy Particle Interactions in Large Targets," Fermilab, 1975.
5. Memo from J. Peoples to Wayne Nestander and Carlos Hojvat, April 28, 1982.
6. M. Barbier, Induced Radioactivity, (Wiley, New York, 1969).

Table 1 - Fortran Geometry Model for
Soil Activation Calculation

```
AX=ABS(X)
AY=ABS(Y)
N=0
IF(X.LE.0.0)GO TO 300
IF(Z.GT.91.4)GO TO 210
IF(RR.GT.14.51)N=2
GO TO 280
210 IF(Z.GT.347.0)GO TO 220
IF(Z.LT.180.0.OR.Z.GT.185.0)GO TO 215
N=1
IF(AX.GT.1.27)N=0
IF(AY.GT.1.27)N=0
215 IF(X.GT.30.48)N=2
IF(AY.GT.45.0)N=2
GO TO 280
220 IF(Z.GT.530.0)GO TO 230
IF(RR.GT.14.51)N=2
GO TO 280
230 IF(Z.GT.713.0)GO TO 240
N=4
IF(AX.GT.7.62.OR.AY.GT.7.62)N=2
GO TO 280
240 N=2
280 IF(AY.GT.106.7)N=3
IF(AY.GT.149.6)N=5
IF(X.GT.213.4)N=3
IF(X.GT.350.0)N=0
GO TO 400
300 IF(Z.GT.91.4)GO TO 310
IF(RR.GT.14.51)N=2
GO TO 380
310 IF(Z.GT.347.0)GO TO 320
IF(Z.LT.180.0.OR.Z.GT.185.0)GO TO 315
N=1
IF(AX.GT.1.27)N=0
IF(AY.GT.1.27)N=0
315 IF(X.LT.-76.2)N=2
IF(AY.GT.45.0)N=2
GO TO 380
320 IF(Z.GT.530.0)GO TO 330
IF(RR.GT.14.51)N=2
GO TO 380
330 IF(Z.GT.713.0)GO TO 340
N=4
IF(AX.GT.7.62.OR.AY.GT.7.62)N=2
GO TO 380
340 N=2
380 IF(AY.GT.106.7)N=3
IF(AY.GT.149.6)N=5
IF(X.LT.-198.)N=3
IF(X.LT.-243.8)N=5
400 CONTINUE
```

*X > 0 is above the beam
Y > 0 is to the right
of the beam (looking
downstream)*

*See text for
list of N values
for different
materials*

List of Figure Captions

1. Plan view of the antiproton target area as of 5/25/82.
2. Elevation view of the antiproton target area as of 5/25/82.
3. Selected plots of Barbier's "danger parameter" for carbon and copper and tungsten as copied from Ref. 6.
4. Contour plots of equal star density as a function of depth Z and radius R for the primary beam transport enclosure upstream of the antiproton target. Also shown is the tunnel and the arbitrary beam elements for the CASIM model. The beam begins to interact at $Z=0$. The vertical scale differs from the horizontal scale.
5. Contour plots of equal star density for the region directly over the target and dump assembly. As in Fig. 4, the enclosure is superimposed on the plots. The vertical scalers differs from the horizontal scale.
6. Cross sectional view of the area near the target showing the diagonal shielding problem.

7. CASIM contour plot for the situation shown in Fig. 6.
8. Plots of energy deposition density for indicated radial bins as a function of Z. The beam profile was a Gaussian with $\sigma = 0.01$ cm.
9. Plots of energy deposition density for indicated radial bins as a function of Z. The beam profile was a Gaussian with $\sigma = 0.038$ cm.
- 10 Plot of enthalpy reserve for various materials as copied from Ref. 1.

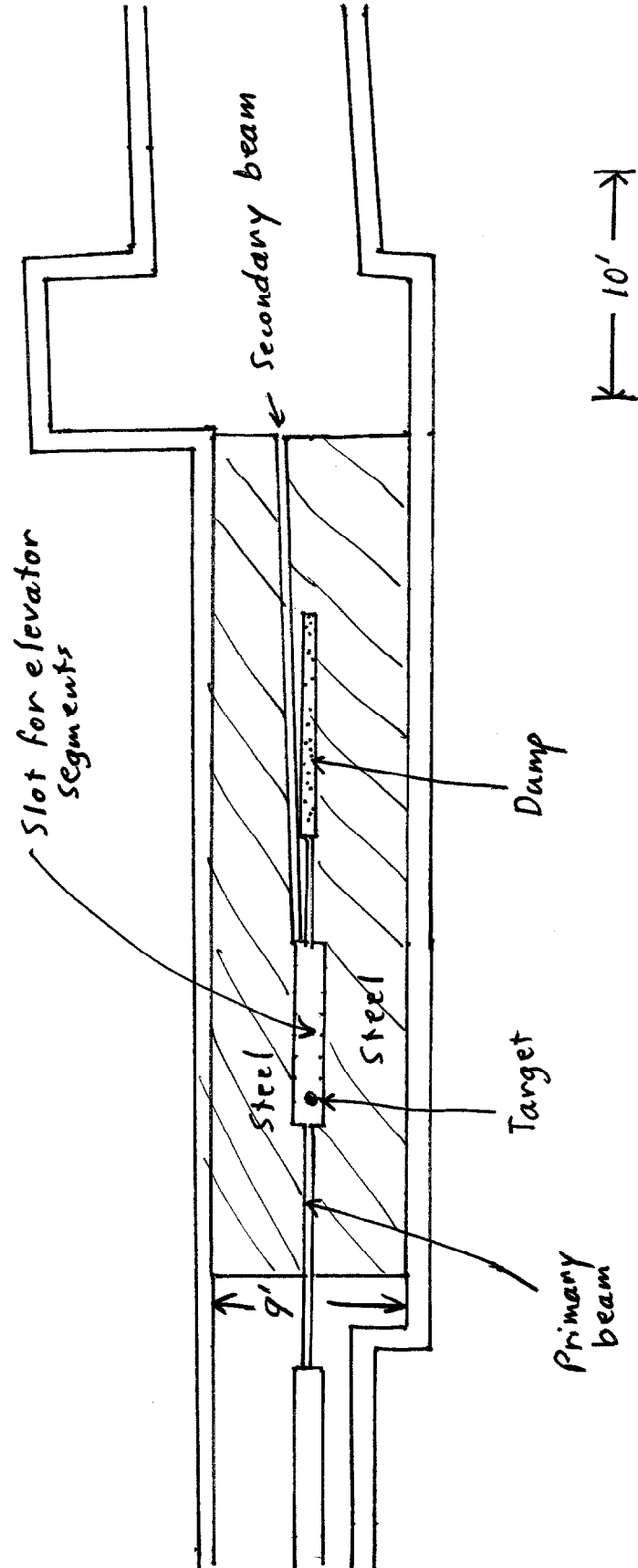
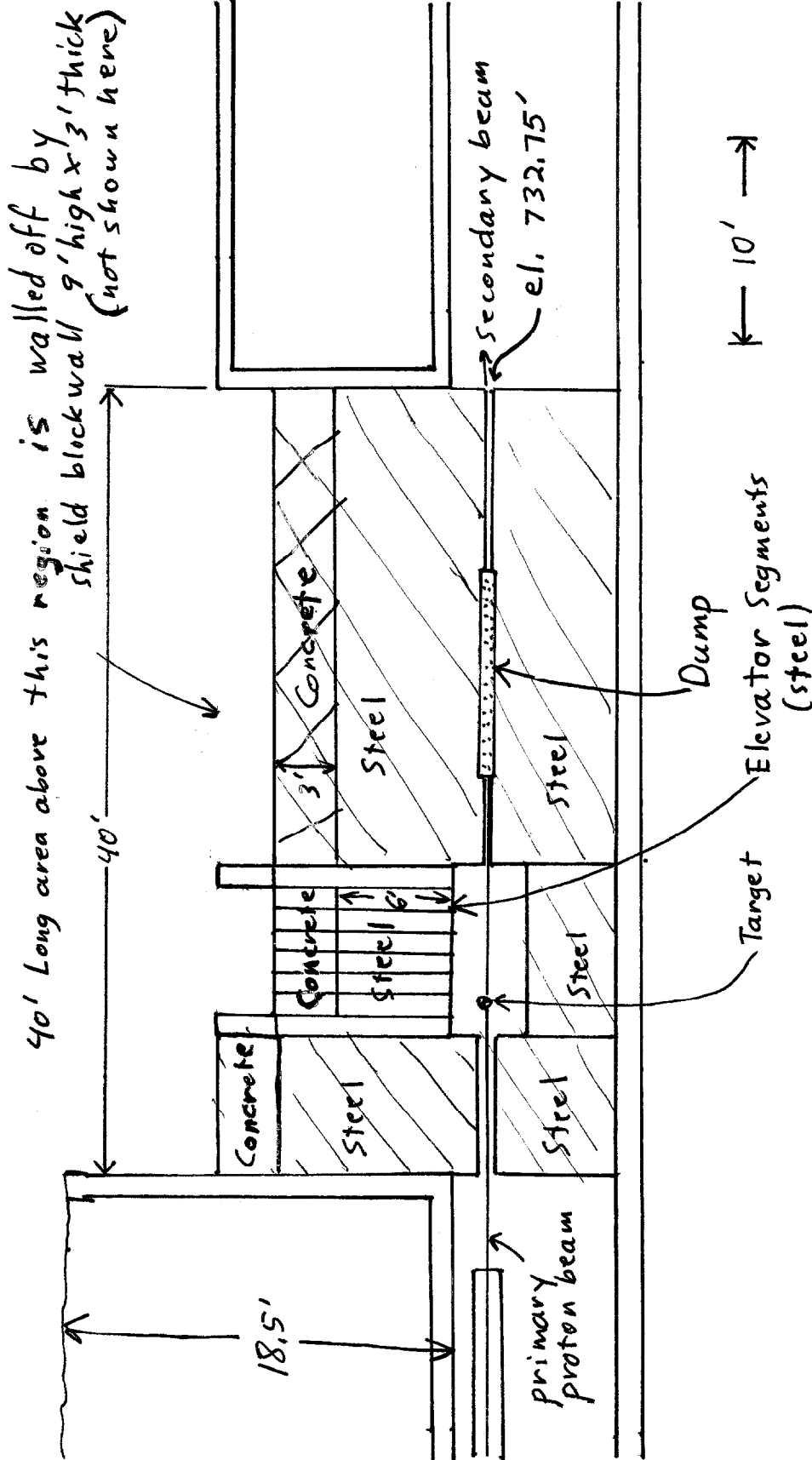


Figure 1 Plan View of Antiproton Target Hall
(in plane of beam)



Elevation View of the Antiproton Target area as of 5/25/82

Figure 2

Fig. B.20

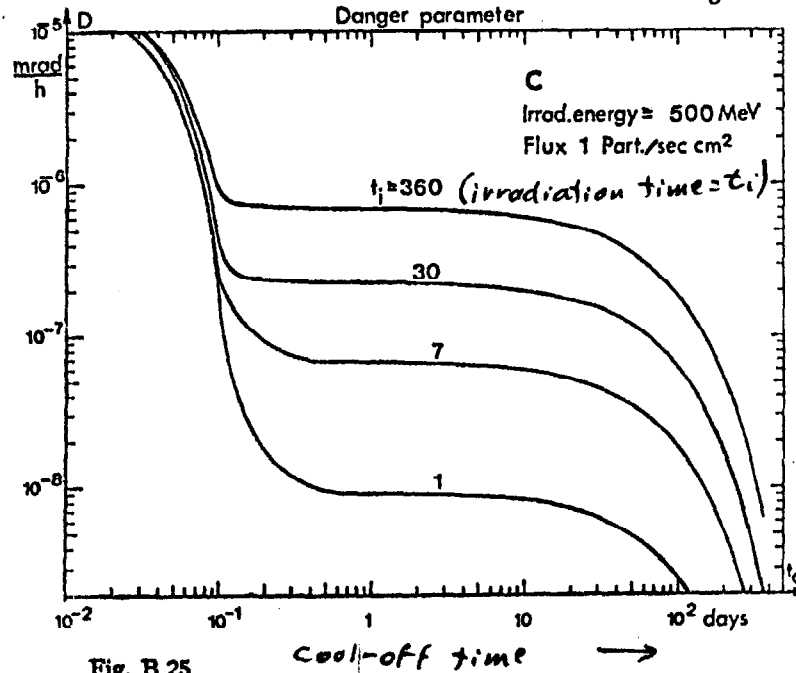


Fig. B.25

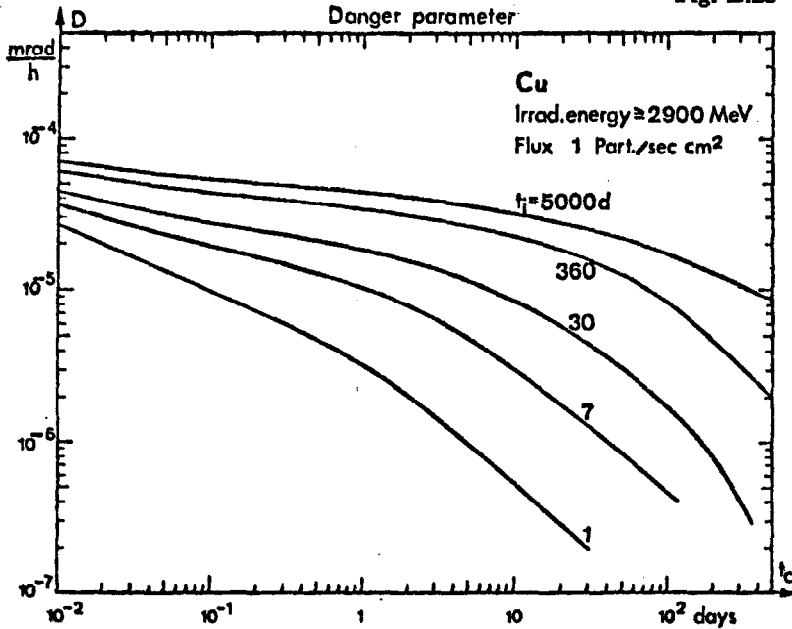


Fig. B.27

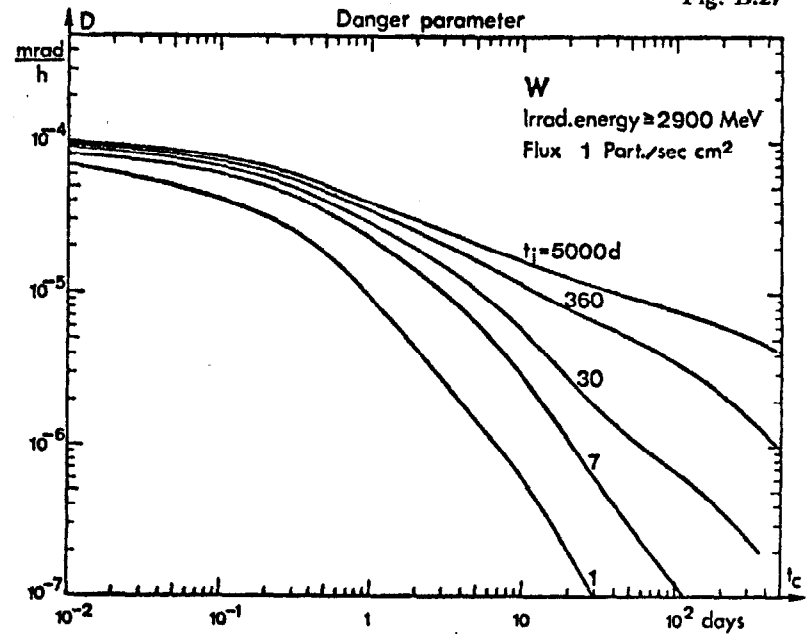


Fig. 3 Selected plots of Barbier's "danger parameter" for Carbon, copper, and tungsten as copied from Ref 6

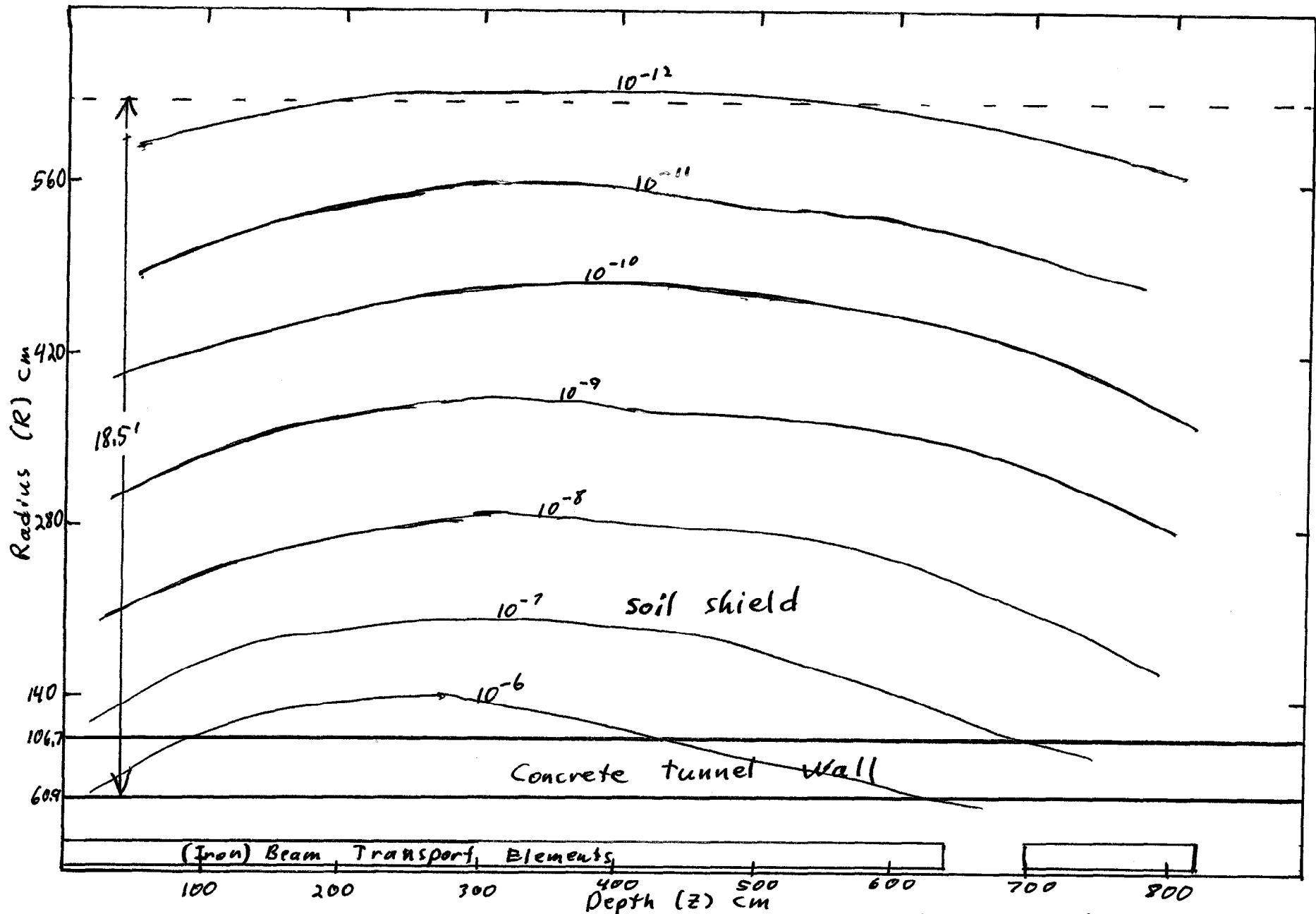


Figure 4 Contours of equal star density (stars $\text{cm}^{-3}/\text{incident proton}$). Beam is scraped on magnets at 8 milliradians beginning at $z=0$. The spot is a Gaussian with $\sigma = 0.5$ cm. This is for accidental loss in the beam transport enclosure.

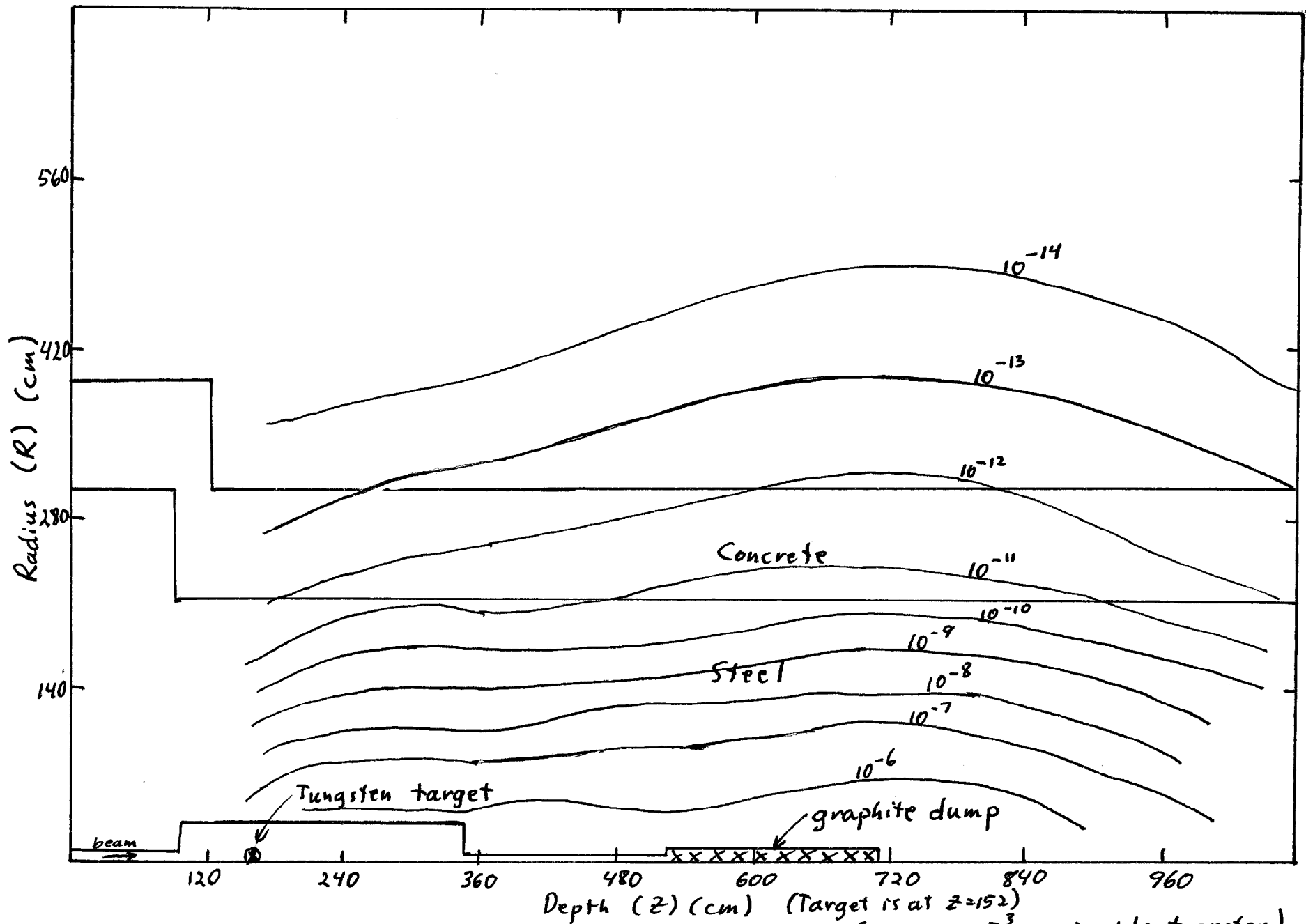


Figure 5 Contour plot of equal star density (stars cm^{-3} per incident proton) for region directly over target and dump. A longitudinal section of the geometry is superimposed on these plots.

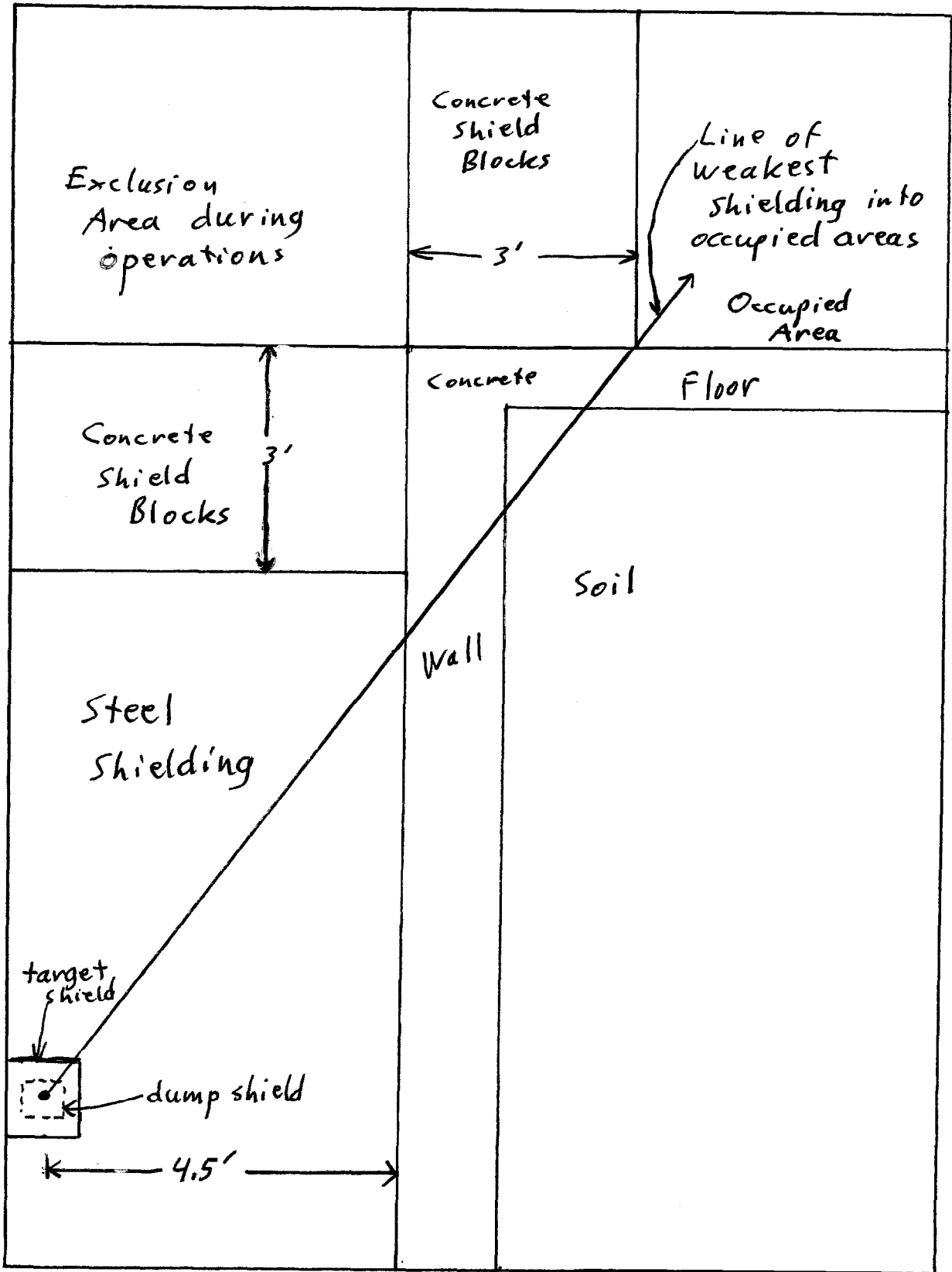


Figure 6 Cross sectional view showing the diagonal shielding problem.

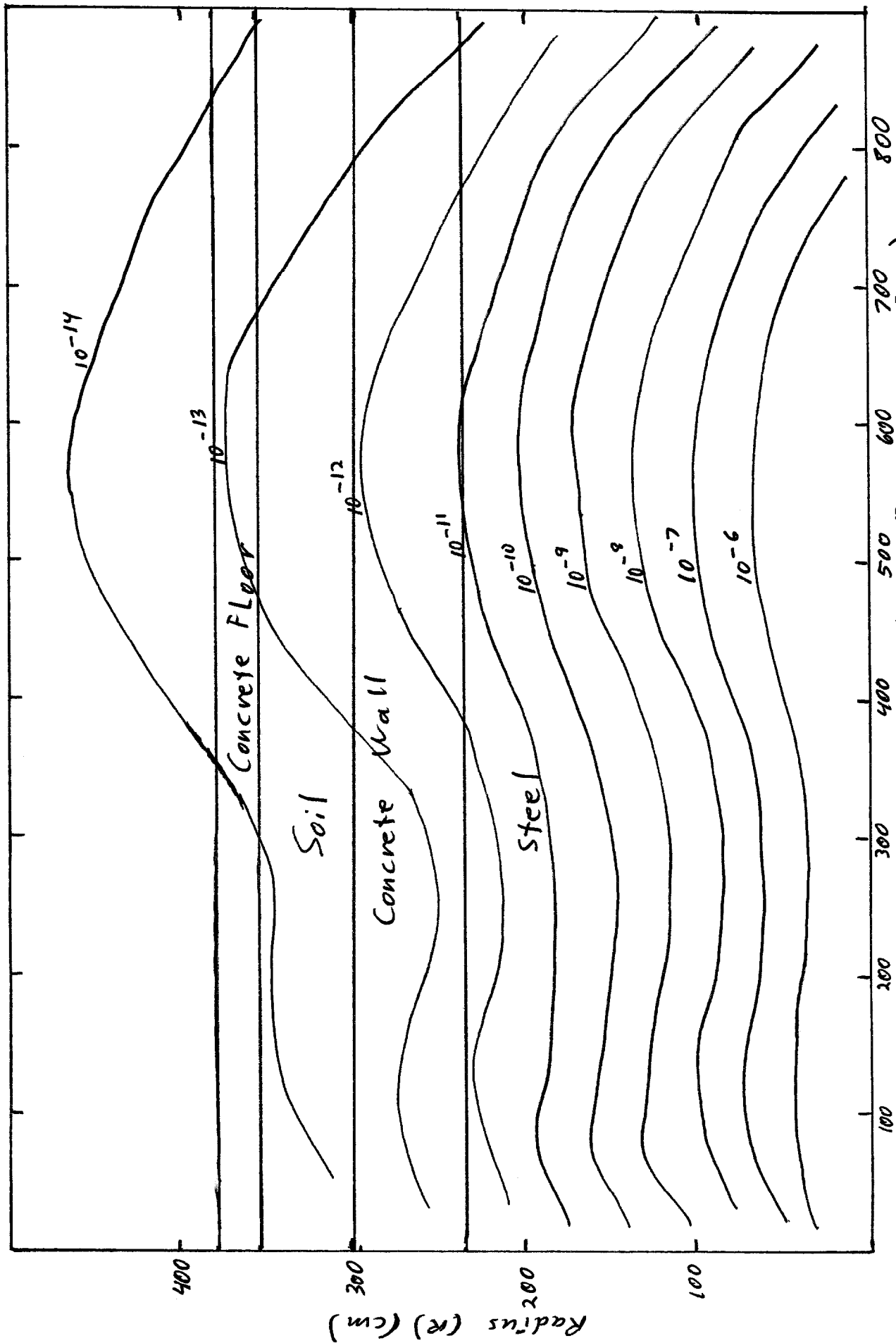
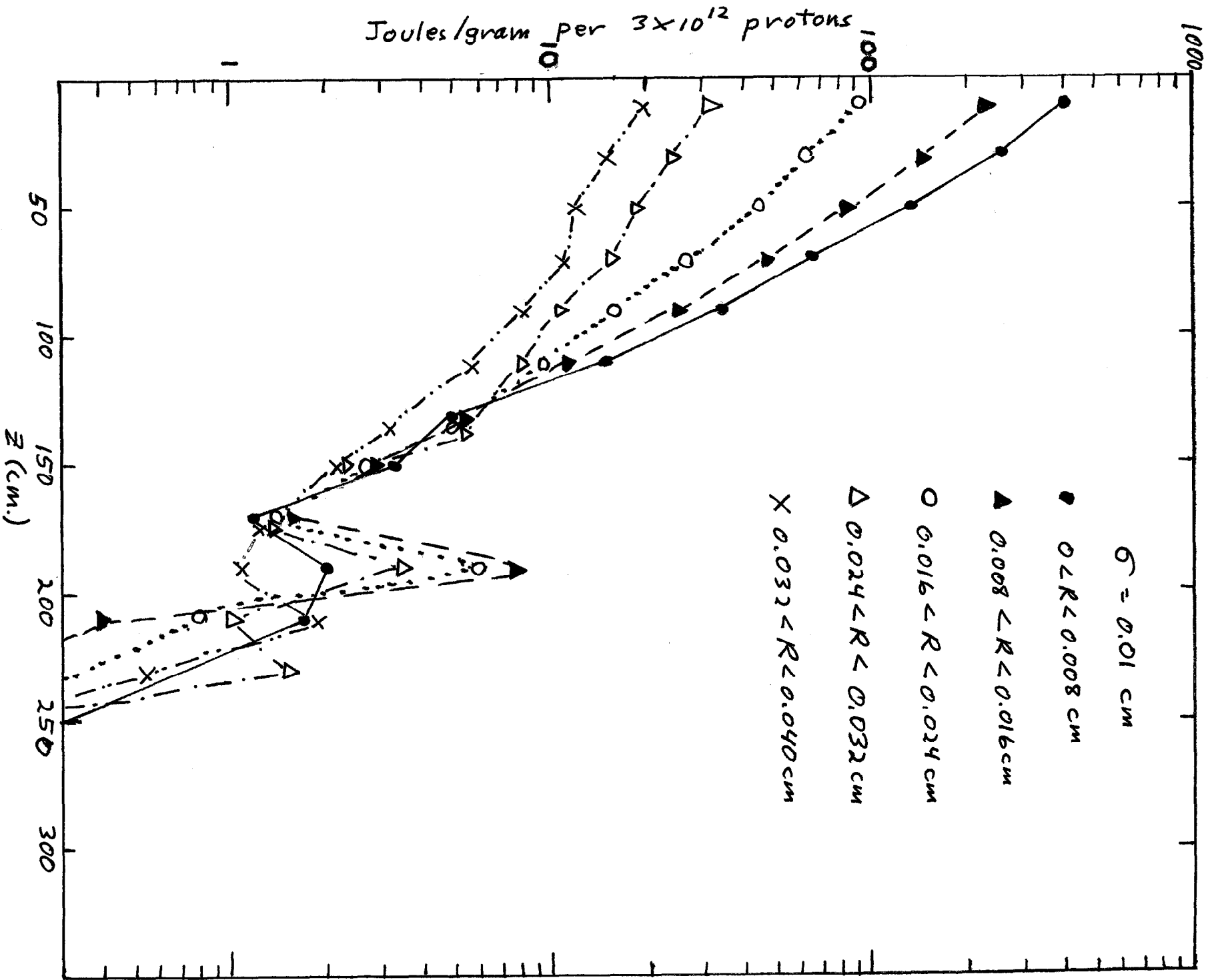
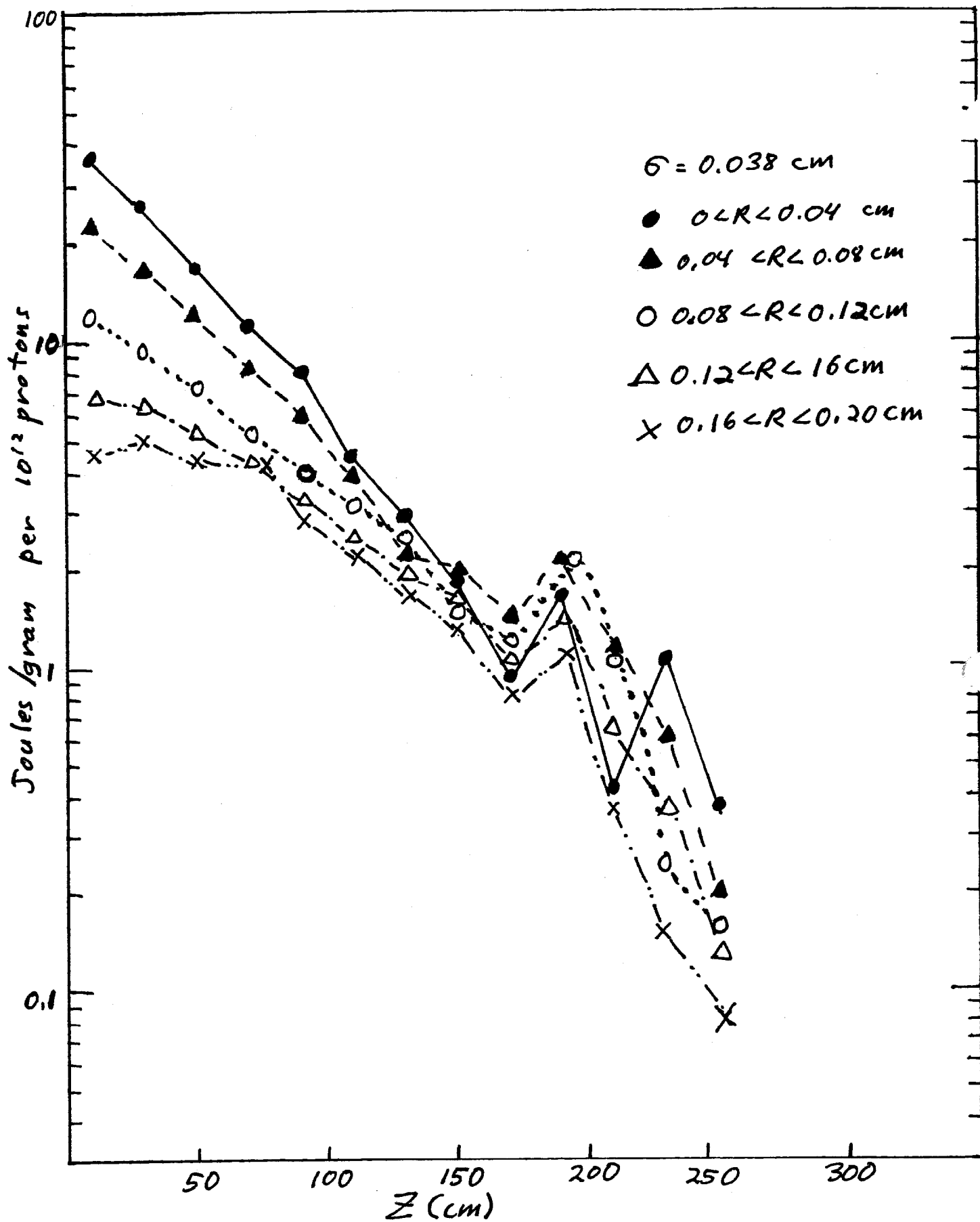


Figure 7
Contour plot of equal star densities using a cylindrically symmetric geometry in which material boundaries were taken radially to be those on the "line of weakest shielding" in Fig. 6.
Depth (Z) cm (Target is at $Z=0$)



Plots of energy deposition / 3×10^{12} protons
in the graphite beam dump. $\sigma = 0.01$ cm

Figure 8



Plots of energy deposition / 3×10^{12} protons
in the graphite beam dump. $\sigma = 0.038 \text{ cm}$

Figure 9

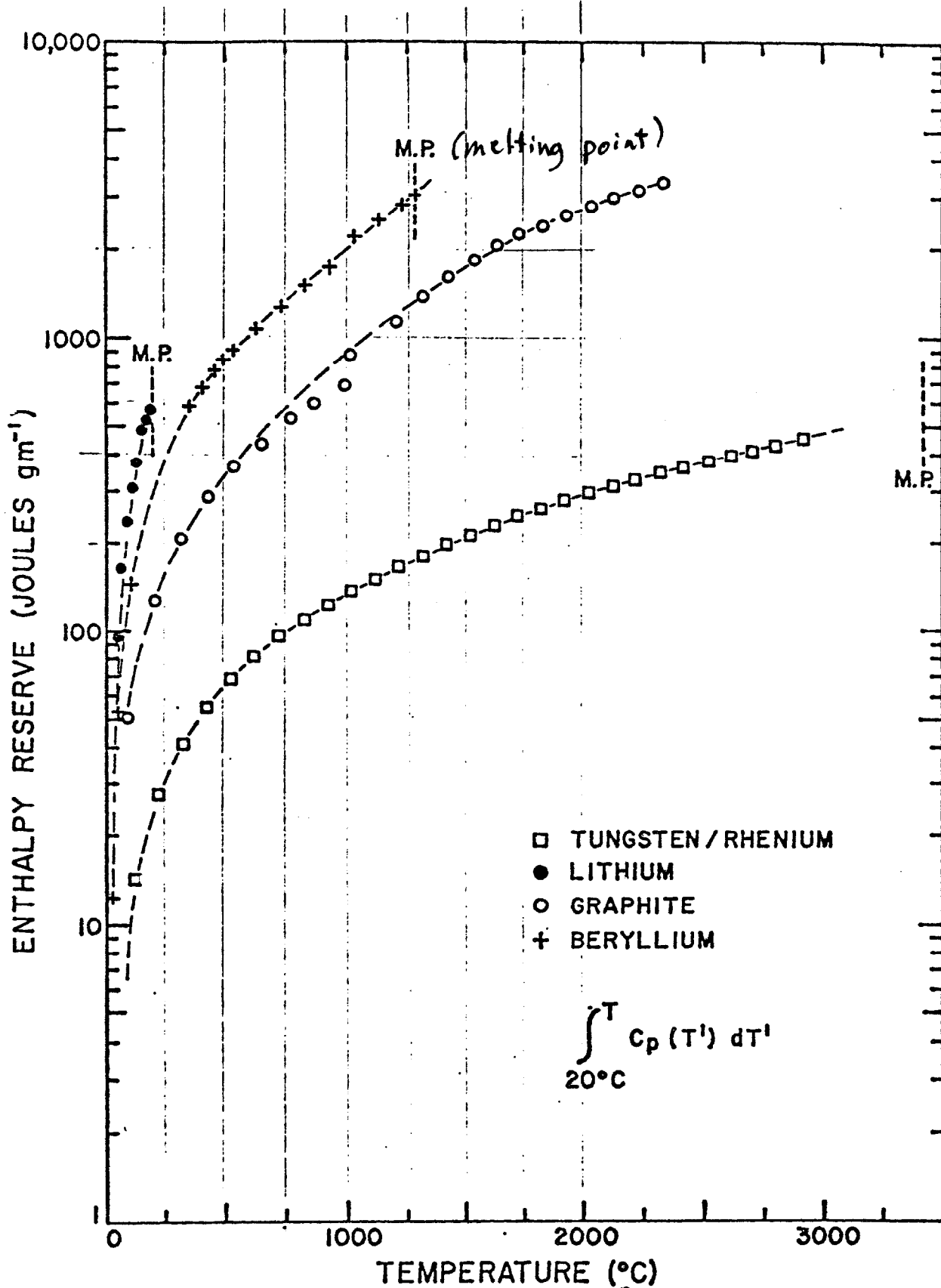


Fig. 3-9 Enthalpy Reserve for Several Materials
Figure 10 (Copied from Ref 1)